TASK QUARTERLY 2 No 2 (1998), 287-317

NUMERICAL SIMULATION OF THE BLADE CASCADE FLOWS USING UPWIND METHODS

TADEUSZ CHMIELNIAK AND WŁODZIMIERZ WRÓBLEWSKI

Institute of Power Machinery
Silesian Technical University
Konarskiego 18, 44-100 Gliwice, Poland

Abstract: In this paper a mathematical formulation of the equations of the fluid motion in turbomachinery cascades has been presented. Some review of the calculation methods for solving these equations is given. These methods are based on an explicit time marching scheme with finite volume discretisation and upwind-biased technique for the inviscid fluxes calculations. The high order accuracy in space is realized by the MUSCL approximation. The discretisations methods and numerical grids are described. The calculations of viscous and inviscid flow models are performed. The model and results of the water steam flow analysis with homogeneous condensation are presented. The calculations are performed for complex problems of real blade configurations of turbomachinery.

1. Introduction

The flow field is modelled by means of a system of three-dimensional, unsteady Navier-Stokes equations describing the laws of the conservation of mass. momentum and energy. If this system of equations is supplemented by constitutive relations and the dependence of the tensor of shear stresses, we get a closed system of equations which can be solved provided the boundary conditions are given. Unfortunately, however, due to the complex character of these equations it is practically not much possible to solve Navier-Stokes equations analytically, except for some very simple cases.

Thanks to the continuous development of computer techniques it has become possible to solve wider and wider classes of problems in the field of fluid mechanics. The beginning of a new field of knowledge, i.e. Computational Fluid Dynamics (CFD), is considered to reach back to the late sixties, when it became possible to make use of extremely quickly operating digital computers. Since that time a constant development of numerical methods has been observed, the requirements concerning the applied models and the calculation efficiency of the computers are growing. Thus, the role of CFD in the designing of aerodynamic elements both in

aircraft engineering and in the case of turbomachines constantly increases. At present numerical investigations are considered to be equally important to theoretical and experimental ones. If, practically, nowadays experimental investigations are still the fundamental way of checking and improving the design of machines and installations, CFD enables us to choose the adequate elements or even complete parts of a turbomachine.

So far in the range of CFD various stages of development have been achieved in the modelling of flow phenomena. As far as the stationary flow is concerned, three-dimensional calculations of turbulent flows can be carried out, applying supercomputers, although it is generally known that the physical models applied at present cannot render fully the reality as it is. Due to the high costs and long time of calculations practically the three-dimensional inviscid flows or quasi-three-dimensional viscous flows models are being carried out. Moreover, papers have already been published dealing with the modelling of unsteady flow phenomena in the complex geometry of turbomachines, making use of a model of viscous gas. In spite of differences which still exist between numerical calculations and reality, the application of the CFD technique makes it possible to obtain a lot of information concerning flow phenomena (e.g. shock waves, boundary layer, the effect of tip clearance and leakage flows, aerodynamic traces, vortexes).

The final aim of all those who deal with numerical fluid mechanics all over the world is to construct a numerical method which would effectively and accurately integrate full Navier-Stokes equation. As far as modelling of a laminar flow is concerned, generally no numerical difficulties have been encountered, and thus no further fundamental investigations are required to find a numerical solution. The application of the laminar flow model is, however, limited because in most technical processes we have to do with turbulent flows, in the case of which full N-S equations are required, but in order to solve them integration ought to be used in a respectively small scale of space and time, which would make it possible to find the non-stationary fluctuations of the flow parameters. Such a numerical procedure would require a large memory and efficiency of the computer. It has been reckoned that a simple example of the flow through a straight duct would require $n^3 = Re^{2.4}$ points in one direction, which would correspond to $n^3 = 240^3$ points (Manna,1992). This quantity is too large even for the best computers. Such a restriction of calculation abilities is the main cause why at present these methods cannot be applied to solve such problems. The best approximation with respect to the possibility of technical applications in modelling of turbulent flow can be achieved by means of Reynolds-averaged Navier-Stokes equations, where the considered conservation equations are being averaged in the characteristic interval of time. The obtained equations are formally identical with equations concerning the laminar flow, except some additional elements, called Reynolds stresses, which have to be modelled. In the course of the past score of years a lot of various models of this kind have been developed. Most of them are based on the conception of the mixing

length of Prandtl, which effectively relates the shear stresses to the gradient of the main velocity (e.g. Merz et al., 1995, Benetschik, 1991)

The highest level of modelling Reynolds stresses was achieved thanks to the application of transport equations for turbulent kinetic energy and its dissipation (model k-ε) (e.g. Chien, 1982; Turner and Jennions, 1992; Lücke et.al., 1995). The next level was reached when a model of Reynolds stresses was applied, assuming a direct modelling of the components of the tensor of Reynolds stresses. All these methods doubt try to supplement the scarcity of information concerning the physical mechanisms of the production and destruction of turbulence, the reason of weak quantitative effect of modelling the turbulent flow.

One level lower in the hierarchy of the equations of motion come Euler equations, describing the inviscid flow. In some cases the solution of these equations may be more difficult than to solve the N-S equations due to the absence of physical dissipation, which plays an important role because it stabilises the numerical algorithm and also due to the possibility of occurrence of the discontinuity in the solution .

The development of calculation algorithms based on the solution of the Euler equations resulted in the elaboration of the methods which differ from each other both with respect to the form of the equations, the method of the discretisation and the applied calculation mesh. While considering problems connected with transonic flows in which shock waves may occur, it is necessary to use the conservative form of Euler equations.

To the most frequently applied methods of calculation belong the finite difference method and the finite volume method. Although the finite difference method was applied first, nowadays the latter one is preferred, particularly in relation to the complex geometry of the flow ducts.

From among the numerical methods from the viewpoint of the discretisation of equations, two groups are to be distinguished: the method of central differences and the "upwind" method. To the most frequently applied method of finite differences belongs Lax-Wendroff method. In this group MacCormack method was especially popular (MacCormack, 1969). The methods of finite differences take into consideration additional elements of dissipation in order to preserve stability. Thus numerical oscillation may be dumped. This leads, however, to a smearing of shock waves into several points of the grid. In literature numerous formulae have been suggested for the determination of artificial dissipation. A comparatively wide application of the method forwarded by Jameson et al. (1981) and Pulliam (1986) has found, in which dissipation of the second and fourth order was introduced. The respective formulae describing the elements of dissipation are more or less complex and often use some empirical parameters. Therefore their range of application is rather limited and requires considerable experience on the part of the user.

An alternative method is the "upwind" method, which is based on the physical properties of the flow. In recent years the "upwind" methods have been developed

extensively. The first to propose this way of discretisation were Courant, Isaacson and Rees (1952). But some enlargement of this method to an non-linear system of equations of the hyperbolic type was put forward by Godunov (1959). In his approach Godunov applied solution of the Riemann problem determining the parameters between the nodes of the grid. This very original approach has found many imitators (e.g. Osher and Solomon, 1982; Roe, 1981; Godunov, 1976; Pandolfi, 1984) and in result we now distinguish a special sub-group of the "upwind" method, the so-called Godunov methods. These have also become known as methods with Flux Difference Splitting (FDS). In contradistinction to finite differences the "upwind" scheme takes into account the characteristic directions of the propagation of disturbances in the flow. Thus it becomes possible to eliminate artificial additional dissipation terms from the calculation algorithm. Thanks to the better consistency of this method with the physical principles it has become possible to model wave phenomena with a complex structure.

In recent years a further progress has been observed, which enables us to determine with good accuracy such distinct wave phenomena as shock waves and tangential discontinuities without unnecessary numerical oscillations. Thanks to the application of the extrapolations in the balance of fluxes the accuracy of this method can still be increased. The application of limiting functions in the extrapolating formula permits to obtain numerical scheme with TVD properties (Total Variation Diminishing) characterised by a monotone decrease of the gradient of values in such a solution and enable us to take into account the discontinuities in the solutions without oscillations..

Most problems connected with the flow of a medium in geometrically complex areas are solved basing on the assumption that we have to do with a model of ideal gas. Applied technically, however, in some cases such a model might prove to be insufficient.

It is widely known that during the expansion of steam from its overheated state the last several stages of an LP part of turbine operate below the saturation line. This causes a deviation of the steam parameters from equilibrium, a decrease of efficiency and finally blade erosion may be possible due to wetness. The non-linear relation between the thermal parameters of state in the superheated region, particularly that near the saturation line, is the most important reason for the application of the real-gas equation of state in calculations of the flow of steam. Other reasons are the respective individual properties of water vapour at and below the saturation line, the possibility of the two-phase structure and the necessity to calculate the thermodynamic parameters and function as accurately as possible in order to get to know exactly the point of expansion (especially in the case of rapid nucleation).

The application of the real gas equation of state in the numerical diagram is more complicated than in the case of ideal gas. An interesting method of solving exactly the Riemann problem for real gas was proposed by Saurel et al. (1994). Euler's governing equation is combined with the system of partially differential equations describing the liquid phase (Schnerr et al., 1989). There is no slip between the vapour and water droplets. Most authors have modelled the flow of water

vapour with phenomena of condensation and solved the equilibrium equations by means of an ideal gas model (e.g. Sejna and Lain. 1994). The modelling of the properties of water vapour and functions in all the flow regions makes it possible to display the condensation process more accurately.

An important element in the solution of the actual flow problem is the discretisation of the calculation domain, which means that the physical area is replaced by a calculation grid. The method of the discretisation of this domain into isolated points called the nodes of the grid is of essential importance for the getting of a correct solution. Nowadays a considerable progress is to be observed in the techniques of numerical grid generation, as well as a large variety of solutions adapted to this problem. The calculation cells are defined depending on the applied numerical methods.

2. Governing Equations

The equation of motion of the fluid can be presented as follows:

$$\frac{\partial Q}{\partial \tau} + L(Q) = H \tag{2.1}$$

The operators $L(Q)$ and values H depend on the flow model, form of dependent variables of the vector Q and coordinate systems applied. In the turbomachinery calculations equation (1) is solved oft in the relative frame of reference rotating with the angular velocity Ω about the z axis with the absolute velocity components (u, v, w) used in the dependent variables.

The the Reynolds-averaged unsteady Navier-Stokes equations obtained from (1) written in a conservative form transformed from the Cartesian coordinate system (x, y, z) to the general curvilinear coordinate system (ξ, η, ζ) with the determinant of Jakobi matrix $J = |\partial(x, y, z) / \partial(\xi, \eta, \zeta)|$ gives:

$$\frac{\partial \hat{Q}}{\partial t} + \frac{\partial \hat{E}}{\partial \xi} + \frac{\partial \hat{F}}{\partial \eta} + \frac{\partial \hat{G}}{\partial \zeta} = \frac{1}{Re}\left[\frac{\partial \hat{E}_v}{\partial \xi} + \frac{\partial \hat{F}_v}{\partial \eta} + \frac{\partial \hat{G}_v}{\partial \zeta}\right] + \hat{H} \tag{2.2}$$

where

$$\hat{Q} = J(\rho, \rho u, \rho v, \rho w, e)^T$$

$$\hat{E} = J\begin{pmatrix} \rho U' \\ \rho u U' + \xi_x p \\ \rho v U' + \xi_y p \\ \rho w U' + \xi_z p \\ e U' + pU \end{pmatrix}, \quad \hat{F} = J\begin{pmatrix} \rho V' \\ \rho u V' + \eta_x p \\ \rho v V' + \eta_y p \\ \rho w V' + \eta_z p \\ e V' + pV \end{pmatrix}, \quad \hat{G} = J\begin{pmatrix} \rho W' \\ \rho u W' + \zeta_x p \\ \rho v W' + \zeta_y p \\ \rho w W' + \zeta_z p \\ e W' + \zeta W \end{pmatrix}$$

$$\hat{H} = (0,0, -\rho\, w\Omega, \rho\, v\Omega, 0)^T$$

Here ρ is the density, p is the pressure, e is the total energy per unit volume. In these equations contravariant relative velocity components are described as:

$$U' = \xi_x u + \xi_y (v + \Omega z) + \xi_z (w - \Omega y)$$
$$V' = \eta_x u + \eta_y (v + \Omega z) + \eta_z (w - \Omega y)$$
$$W' = \zeta_x u + \zeta_y (v + \Omega z) + \zeta_z (w - \Omega y)$$

and contravariant absolute velocity components as:

$$U = \xi_x u + \xi_y v + \xi_z w$$
$$V = \eta_x u + \eta_y v + \eta_z w$$
$$W = \zeta_x u + \zeta_y v + \zeta_z w$$

The viscous terms are given assuming no internal energy sources or radiation heat transfer as:

$$\hat{E}_v = J \begin{pmatrix} 0 \\ \xi_x \tau_{xx} + \xi_y \tau_{xy} + \xi_z \tau_{xz} \\ \xi_x \tau_{yx} + \xi_y \tau_{yy} + \xi_z \tau_{yz} \\ \xi_x \tau_{zx} + \xi_y \tau_{zy} + \xi_z \tau_{zz} \\ \xi_x E_{ev} + \xi_y F_{ev} + \xi_z G_{ev} \end{pmatrix}, \quad \hat{F}_v = J \begin{pmatrix} 0 \\ \eta_x \tau_{xx} + \eta_y \tau_{xy} + \eta_z \tau_{xz} \\ \eta_x \tau_{yx} + \eta_y \tau_{yy} + \eta_z \tau_{yz} \\ \eta_x \tau_{zx} + \eta_y \tau_{zy} + \eta_z \tau_{zz} \\ \eta_x E_{ev} + \eta_y F_{ev} + \eta_z G_{ev} \end{pmatrix},$$

$$\hat{G}_v = J \begin{pmatrix} 0 \\ \zeta_x \tau_{xx} + \zeta_y \tau_{xy} + \zeta_z \tau_{xz} \\ \zeta_x \tau_{yx} + \zeta_y \tau_{yy} + \zeta_z \tau_{yz} \\ \zeta_x \tau_{zx} + \zeta_y \tau_{zy} + \zeta_z \tau_{zz} \\ \zeta_x E_{ev} + \zeta_y F_{ev} + \zeta_z G_{ev} \end{pmatrix}$$

$$E_{ev} = u\tau_{xx} + v\tau_{xy} + w\tau_{xz} - q_x$$
$$F_{ev} = u\tau_{yx} + v\tau_{yy} + w\tau_{yz} - q_y$$
$$G_{ev} = u\tau_{zx} + v\tau_{zy} + w\tau_{zz} - q_z$$

In the viscous terms $\bar{\tau}$ is a stress tensor and $\vec{q}$ is the heat flux vector.

The concerned equations are incomplete equations system. To solve this set of

equations it is necessary to close it by the equations of state. These equations could be referenced to the ideal gas model or to the real gas (in presented calculations to the water vapour).

Ideal gas

The static pressure with perfect gas equation of state is defined by:

$$p = (\gamma - 1)\left(e - \frac{1}{2}\rho \left(u^2 + v^2 + w^2\right)\right) \tag{2.3}$$

where γ is the ratio of specific heats.

Water vapour

The water vapour equation of state proposed by Wukalowicz (1969) was chosen. It is a virial equation with three coefficients:

$$z = \frac{pv}{RT} \cdot 10^2 = 1 + Bp + Cp^2 + Dp^3 \tag{2.4}$$

were z is a coefficient of compressibility and A, B, C are the virial coefficients only depending on the temperature T.

When we deal with the real gas equation of state the energy has to be calculated from the relation:

$$e = h\rho - p + \frac{1}{2}\rho \left(u^2 + v^2\right) \tag{2.5}$$

where h is the enthalpy of the real gas.

In this case enthalpy of the water vapour equals:

$$h = h_g \cdot (1 - y) + h_l \cdot y \tag{2.6}$$

where h_g denotes the enthalpy of the vapour phase, superheated vapour calculated from the Wukalowicz relations (Wukalowicz 1969) and h_l denotes the enthalpy of the liquid phase. In the equation above y denotes the non-equilibrium wetness fraction calculated from the equation proposed by Dejcz (1981) with equation of droplets growth obtained from the kinetic theory of gases (Chmielniak et al, 1997).

For viscous flows calculations additionally the transport quantities are required. These quantities are obtained for laminar flow from the linear relationship between shear stresses and velocity gradient, and between heat flux and temperature gradient. For turbulent flows the turbulence model should be used. The very popular in the turbomachinery calculations is the Baldwin-Lomax model which is the two-layer algebraic model (Baldwin and Lomax, 1978).

3. Domain Discretisation. Computational Grid

The kind of the applied discretisation of the flow domain, i.e. the generation of a numerical mesh, affects the quality of the results of calculations to a considerable extent. An essential element is its adaptation to the considered calculation problem in

order to obtain adequate results.

To the fundamental types of grids applied in fluid mechanics belong regular grids, irregular grids, and also adapted grids.

As far as regular grids are concerned we distinguish three types "*O*", "*C*" and "*H*", depending on the shape of the two families of intersect curves, with defining grids. The latter one is of particular importance, as those curves define the boundary of the calculation domain. Examples of fundamental regular meshes may be seen in Figures 3.1, 3.2, 3.3. The generators of these grids are based on the solution of elliptical differential equations (Soerenson 1980, Thompson et al. 1974, Wróblewski and Górski 1992).

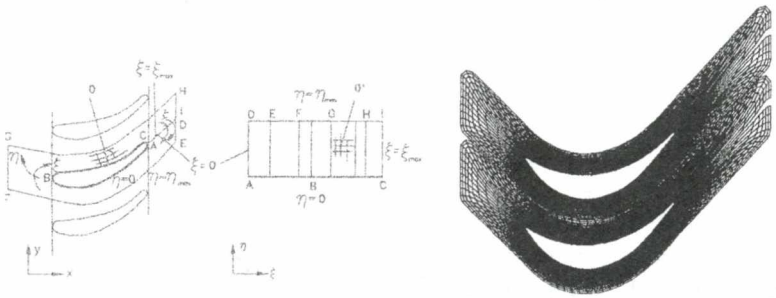

Figure 3.1 *"O"-type grid (a-transformation,b-example)*

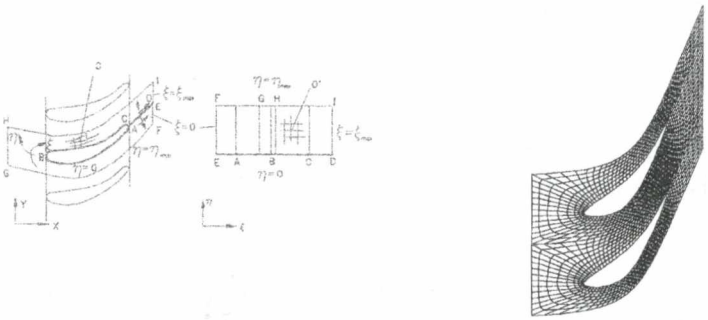

Figure 3.2 *"C"-type grid (a-transformation,b-example)*

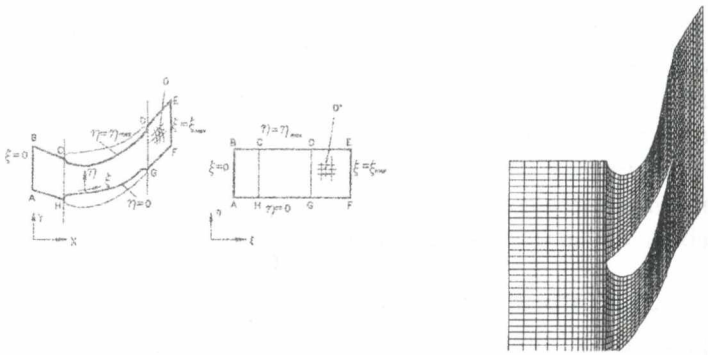

Figure 3.3 *"H"-type grid (a-transformation,b-example)*

Although not universal, these regular grids are most frequently used to calculate the flow in turbomachines.

Numerical grids must display several properties warranting correct results, viz.:

- One-to-one mapping
- Orthogonality - in the case of complex geometry it should be attempted to reach a possibly maximum orthogonality. The grid generation requires at each point extremely complex algorithms, as well as a high efficiency of the computer,
- Smoothness,
- Automatic generation,
- Adaptation to the requirements of the given problem. The possibility of adapting the density of the mesh to the predicted gradients of the flow parameters is of essential importance for the accuracy of the obtained results of calculations.

From the viewpoint of calculations, the area of aerodynamic traces behind the profile is quite well discretised by grids of the type "*C*". Such grids are, however, rather sensitive to the geometry of thick and strongly curved profiles. In spite of these difficulties this type grids are widely used to calculate internal flows.

Some defects of "*C*"-type grids can be eliminated by the application of "*O*"-type grids. The latter provide more possibilities to discretise the leading edge and trailing edge of the profile. Their drawback, however, is the presence of large grid cells at some distance from the inner boundary.

The "*H*"-type grid is comparatively often used in calculations, owing its popularity to the fact that it can be easily adapted to any shape of the duct. The main drawback of this type of grids is the poor discretisation of the inlet edge causing numerical "losses" in calculations of the flow.

In irregular grids their points are not identified with only one line of the co-ordinate system. These grids are more elastic in the case of complex (combined) geometry, although the local arrangement of the co-ordinates complicates the algorithm of the solution considerably and increases the requirements concerning the efficiency of calculation of the computers.

The most important field of the development of the grid generation methods is the development of the system of dynamic adaptation, where the grid points can be relocated in the course of calculating the flow, depending on the existing physical phenomena. The application of these grids makes it possible to attain a good distribution while modelling the discontinuities in the flow. Their drawback is the complex algorithm of computation and A much longer time of solving the given problem.

4. Numerical Scheme

The algorithm used to solve the system of equations (2.2) is a time-marching method. The discretisation in space of the flow gradients was carried out using the node-centered finite volume method (Figure 4.1). The explicit, first order accurate

forward time integration is implemented. The algorithm for the viscous flow calculation consists of inviscid and viscous parts. The inviscid part is the same as for the calculation of the inviscid flow model.

For the inviscid part the numerical form of the equation (2.2) is:

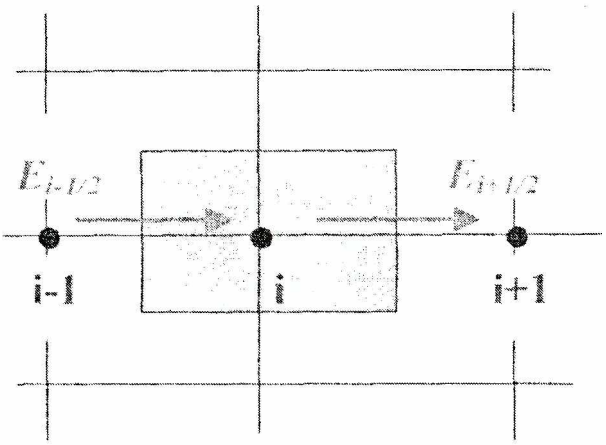

Figure 4.1 *Node-centered finite volume. Fluxes in the x direction*

$$\hat{Q}^{n+1}_{i,j,k} = \hat{Q}^{n}_{i,j,k} - \Delta t\left(\hat{E}^{n}_{i+1/2,j,k} - \hat{E}^{n}_{i-1/2,j,k} + \hat{F}^{n}_{i,j+1/2,k} - \hat{F}^{n}_{i,j-1/2,k} + \hat{G}^{n}_{i,j,k+1/2} - \hat{G}^{n}_{i,j,k-1/2}\right) \quad (4.1)$$

Numerical fluxes on the cell boundaries have to be calculated to obtain the solution of eq.4.1.

4.1. Flux calculation

Fluxes on the calculation cell boundary e.g. $E_{i+1/2}$ for direction x (Figure 4.1), are functions of the conservative variables defined in the adjacent nodes:

$$E_{i+1/2} = E_{i+1/2}\left(Q_{i-1}, Q_i, Q_{i+1}, Q_{i+2}\right) \quad (4.2)$$

The one of the interpolation method should be chosen to calculate the flux value on the interface. The central difference and upwind methods are widely used for the flux calculation on the cell boundary. The fluxes in the other directions are determined in the same manner.

Central difference method

In the second-order accuracy central difference scheme the simple averaging method is used. For the non-linear equations two averaging methods are proposed:

$$E_{i+1/2} = E\left(\frac{Q_i + Q_{i+1}}{2}\right), \qquad E_{i+1/2} = \frac{E(Q_i) + E(Q_{i+1})}{2} \quad (4.3)$$

In both of the cases the consistency condition in the limit $\Delta x \to 0$ have to be fullfield.

The central difference schemes are characterised by the following properties (Hänel, 1993):

- generally second-order accuracy in space,
- consider the influence of perturbations with negative and positive characteristics,
- some kind of separation of even- and odd- numbered nodes,
- it is necessary to use dumping terms to avoid oscillations in the solution, especially in the regions where discontinuous appear

In the central-difference methods the dumping terms of second $d^{(2)}$ and fourth $d^{(4)}$ order are used (Jameson et all, 1981). The second order terms eliminate nonlinear oscillations in the regions close to the discontinuous and the fourth order terms eliminate short waves oscillations from the solution. The dumping terms should not influence the solution in the domain with continuous flow parameters. Numerical flux on the calculation cell in this case is described in the form:

$$E_{i+1/2} = \frac{1}{2}\left(E(Q_i) + E(Q_{i+1})\right) + d^{(4)}_{i+1/2} + d^{(2)}_{i+1/2} \tag{4.4}$$

The dumping terms have some empirical parameters which should be adjusted for the examined flow problem in the calculation process. It is a disadvantage of the central difference scheme.

Upwind scheme

In the upwind scheme the dumping terms are eliminated. In this case the fluxes are evaluated as a function of the propagation direction of the disturbance propagation speed. The construction of the upwind scheme is more complicated and the rule of the flux calculation is more complex than in the case of central difference scheme and therefore is much more time consuming.

In the 3-D Euler equations five real characteristics are determined. The forward or backward differencing method is used, depending on the sign of characteristics. It is not possible to formulate one kind of differencing method for all terms of the flux vector E. For this reason in the upwind schemes the flux have to be splitted in to the terms which consider different propagation directions. Among the most popular upwind discretisation methods belong:

1. Flux-Vector Splitting — FVS
2. Flux-Difference Splitting — FDS

FVS

In the Flux-Vector Splitting method flux E is replaced by two terms depending on the parameters in the two adjacent cells and eigenvalue signs as follows:

$$E_{i+1/2} = E^{+}(Q_i) + E^{-}(Q_{i+1}) \tag{4.5}$$

The one of the first FVS scheme was developed by Steger and Warming (1981). The disadvantage of this scheme is the fact that in the stagnation points, sonic points, and points where the eigenvalues change the sign the splitted fluxes are not differentiated. This leads to the oscillations in the solution (Manna 1992).

The method proposed by van Leer (1982) was the next widely used FVS method. In this method the continuous first order difference of the splitted fluxes is preserved due to the approximation polynomial with Mach number as variable. Van Leer scheme works not well in the regions where the shear discontinuity appear (van Leer 1982, van Leer et al. 1987). That was the reason of many improvements in the scheme. More details could be found in works: Schwane and Hänel (1989), Chmielniak (1994).

FDS

The Flux Difference Splitting method was first proposed by Courant, Isaacson, Rees (1952), and next extended for the non-linear problems. In this method the numerical flux is splitted into two terms. The first one is a central difference term and the second one is upwind term. difference. The upwind term in this method makes the discretisation from central difference- to the upwind- type when the values of the characteristics increase. The flux is calculated as:

$$E_{i+1/2} = \frac{1}{2}\left(E(Q_i) + E(Q_{i+1}) - |A|(Q_{i+1/2})(Q_{i+1} - Q_i)\right) \tag{4.6}$$

Matrix $|A|$ is in the form:

$$|A| = L^{-1}|\Lambda|L \tag{4.7}$$

where Λ is the eigenvalue matrix, L is the eigenvector matrix. Matrix A is defined on the cell interface $i+1/2$. The calculation method of this matrix determine the variants of the FDS scheme

The FDS scheme for the non-linear equations was first proposed by Godunov (1959). The flux $E_{i+1/2}$ is defined as:

$$E_{i+1/2} = E(Q_{i+1/2}) \tag{4.8}$$

were the value $Q_{i+1/2}$ on the cell interface is calculated as the solution of the local one-dimensional Riemann problem defined for the parameters in the adjacent cells. The following steps are required:

1. Defining the discrete (piecewise constant) values of conservative variables for time t^n on each cell surface k necessary to formulate local Riemann problems (left and right hand initial states are the values $Q^L_{i+1/2}$ and $Q^R_{i+1/2}$ in the adjacent calculation cells);
2. The exact or approximate solution of the one-dimensional Riemann problem for direction normal to the interface of the cell. Detailed description of this solution is presented by Chmielniak and Wróblewski (1995), Chmielniak et al (1997);

3. The calculation of the numerical fluxes on the cell boundaries and obtaining the averaged solution in time t^{n+1}.

Godunov method approximates a flow by a large number of the constant states, computes their interactions exactly, and averages the results in a conservative fashion. As a consequence of the averaging procedure, much of the details of the Riemann problem solutions could be lost. The main drawback of the methods is the difficulty and the cost of the iterative solution of the non-linear Riemann problem. That has led to various attempts to approximate the Riemann problem. One of the first approximations proposed by Godunov (1976), was to replace all the waves in Riemann problem by sound waves, in cases when the waves were expected to be weak. That in effect amounted to the use of only one iteration in the solution of Riemann problem. In this case the difficulty could appear when the strong waves appear in the flow (e.g. shock waves).

Another simplification of Riemann problem has been developed by Osher (1984), Osher and Solomon (1982).The Osher scheme is based also on the Godunov scheme, but compression and rarefaction waves are used to approximate the shocks. That leads to the similar algorithm. The numerical flux functions, which are the least continuous by differentiable, are written in closed form, and include various switches which make them upwind.

The numerical flux for the Osher scheme is implemented according to the following expressions

$$
\begin{aligned}
E_{i+1/2} &= \frac{1}{2}\left[\left(E_L + E_R\right)_{i+1/2} - \int_{Q_L}^{Q_R} \left\{ \left\{ \frac{\partial E}{\partial Q} \right\}^{+} - \left\{ \frac{\partial E}{\partial Q} \right\}^{-} \right\} dQ \right] \\
&\equiv E_R - \int_{Q_L}^{Q_R} \left\{ \frac{\partial E}{\partial Q} \right\}^{+} dQ \\
&\equiv E_L + \int_{Q_L}^{Q_R} \left\{ \frac{\partial E}{\partial Q} \right\}^{-} dQ
\end{aligned}
\tag{4.9}
$$

The integration path in phase space from Q_L to Q_R is split over either forward (+) or backward (-) moving simple waves.

The approximate Riemann solver developed by Roe is probably the most popular in the gas dynamic calculations. It is based on the characteristic decomposition of the flux differences, while preserving the conservation properties of the scheme. In Roe approach, specially averaged cell interface values are determined for density, velocity and enthalpy. Using these specially averaged values, Roe evaluates the Jacobian matrix and then considers the approximate linear Riemann problem. In this approach the interface flux is:

$$E_{i+1/2} = \frac{1}{2}(E_L + E_R) - \frac{1}{2}\sum_k |\lambda_k| \alpha_k r_k \tag{4.10}$$

where λ_k, α_k and r_k are the eigenvalues (wave speeds), wave strengths, and eigenvectors, respectively (for more details see e.g. Roe 1981, Hirsch 1990).

Roe scheme gives not good enough solutions in the regions where eigenvalue λ_k tends to zero. This results in setting to zero the upwind term of equation (4.10) and the dumping term vanish. This may lead to the non-physical solutions. In this case a eigenvalue correction is needed (e.g.. Harten i Hyman, 1983).

The Osher and Roe schemes allow relatively simple field to field non-linear decomposition of the Riemann problem.

Because in Roe, Osher and Godunov schemes the solution of the one-dimensional Riemann problem is used they are called Godunov-type schemes.

The diffusive terms in the viscous flow calculations are determined using a special central volume (Figure 4.2). To construct the numerical viscous fluxes at the cell interfaces it is necessary to evaluate derivatives of the velocity components. They are treated according to Chakravarthy (1988) and Benetschik (1991).

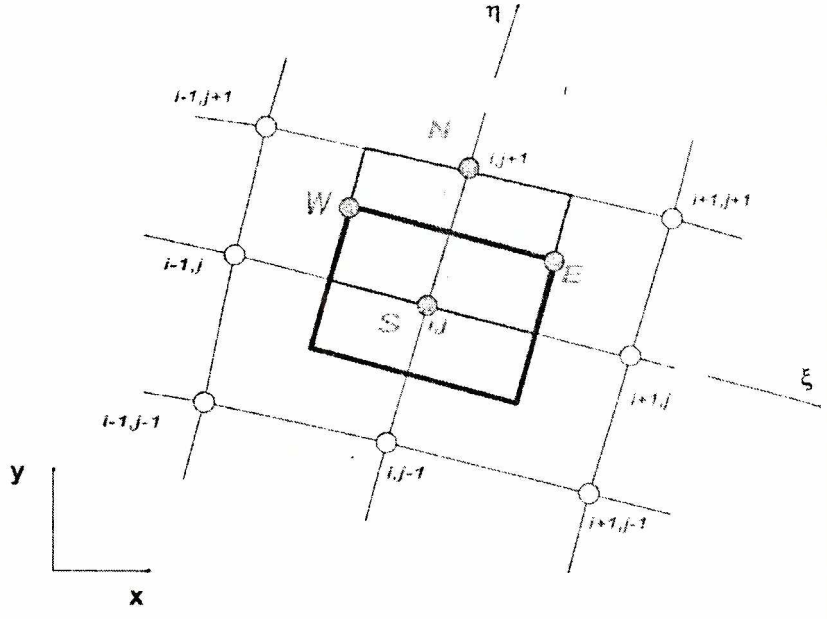

Figure 4.2 *Numerical cell for diffusive terms calculations*

4.2. High order accuracy in space

The classical Godunov scheme leads to monotonic algorithms of the first order accuracy in space. The values from the adjacent nodes are used for defining the Riemann problem or for FVS formulations:

$$Q_L = Q_i$$
$$Q_R = Q_{i+1} \tag{4.11}$$

To obtain higher accuracy of the calculations the interpolation of the node parameters to the cell interface is used.

$$Q_L = Q^L_{i+1/2}$$
$$Q_R = Q^R_{i+1/2} \tag{4.12}$$

To obtain higher accuracy and preserving monotonicity, the MUSCL approximation has been applied (see van Leer, 1979, Hirsch, 1990) with the van Albada limiter function s (van Albada et al., 1982). In this case, the vector of conservative variables is computed from the equation:

$$Q^L_{i+1/2} = Q_i + \left[\frac{s}{4}\left((1-k)\nabla_\xi Q + (1+k)\Delta_\xi Q\right)\right]_i$$
$$Q^R_{i+1/2} = Q_{i+1/2} - \left[\frac{s}{4}\left((1-k)\Delta_\xi Q + (1+k)\nabla_\xi Q\right)\right]_{i+1} \tag{4.13}$$

where

$$\Delta_\xi Q = Q_{i+1} - Q_i$$
$$\nabla_\xi Q = Q_i - Q_{i-1}$$

$$s = \frac{2\Delta_\xi Q \nabla_\xi Q + \varepsilon}{\left(\Delta_\xi Q\right)^2 + \left(\nabla_\xi Q\right)^2 + \varepsilon}$$

The value ε was introduced to avoid division by zero ($\varepsilon = 10^{-5}$). For $k = 1/3$ we obtain the third order accuracy scheme. With the use of the flux limiter the scheme shows properties similar to those of the TVD-schemes. Interpolation can be defined for conservative (ρ, ρu, ρv, ρw, e) or primitive (ρ, u, v, w, e) variables.

4.3. Boundary conditions

Boundary conditions have to be specified on the surfaces presented in Table 4.1. and Figure 4.3. (for 2D case):

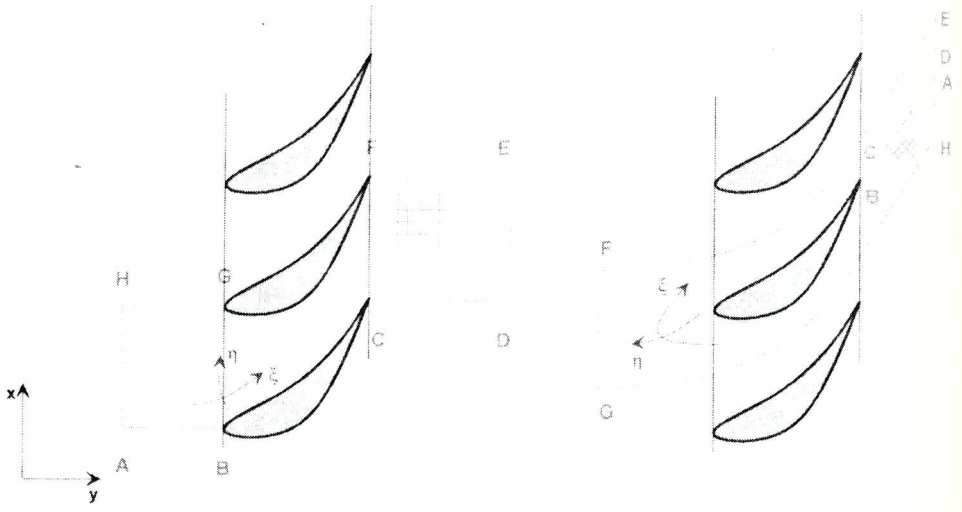

Figure 4.3 *Boundary surfaces:a) "H"-type grid, b) "C"-type grid*

Table 4.1. *Boundary surfaces*

Boundary	"H"-type grid	"C"-type grid
Inlet	A–H	F–G
Outlet	D–E	A–H,D–E
Periodic	A–B,C–D,E–F,G–H	G–H,E–F
Walls	B–C,F–G	B–C

The appropriate choice and the numerical implementation of boundary conditions are very important elements of the whole computation process. The number of the quantities to be specified on the inlet and outlet boundary depends on the characteristic directions defined for the velocity normal to the boundary. For each characteristic running into the calculation domain appropriate physical conditions are specified. For the characteristics running outside the numerical conditions are required (see table 4.2.).

Table 4.2. *Number of physical and numerical boundary conditions.*

Inlet and outlet boundary conditions		***Physical b.c.***		***Numerical b.c.***	
		2D	***3D***	***2D***	***3D***
Inlet	subsonic	3	4	1	1
	supersonic	4	5	0	0
Outlet	subsonic	1	1	3	4
	supersonic	0	0	4	5

At the subsonic inlet for the turbomachinery calculations the following physical quantities are implemented: for 2D case the total temperature, the total pressure and the flow angle and for 3D case the second flow angle is added. The value of Riemann invariant at the inlet boundary

$$R = V' + \frac{2}{\gamma - 1} a \quad \text{for "C" type grid } (\eta = \eta_{\max})$$
$$R = U' - \frac{2}{\gamma - 1} a \quad \text{for "H" type grid } (\xi = 0) \tag{4.14}$$

is determined on the basis of quantities defined for the internal cell adjacent to the boundary. For the supersonic inlet, all components are computed from the physical quantities prescribed on the boundary.

Only one physical variable is added at the subsonic outlet. For the turbomachinery calculations the static pressure is usually assumed. The remaining quantities are computed from compatibility relations for Euler equations. In the 3-D calculations the radial distribution of static pressure at the outlet is calculated from the radial equilibrium equation.

Apart from the discussed boundary conditions, two types of internal conditions remain to be defined: conditions resulting from separation of one passage (periodicity condition), and for stage calculations relations defining the transfer from the stator frame of reference to the rotor one. In the first case, since the flow is examined in the reference system x, y, z, special attention should be paid to an appropriate transformation of component velocities. While defining conditions on the boundary line separating the stator from the rotor, one should use standard boundary conditions at the inlet and outlet, as it has been described above, taking into consideration the relationship between circumferentially averaged parameters in the absolute and relative frame of reference.

For inviscid flow calculations the impermeability condition at solid walls is used. Detailed description of boundary conditions used for the Euler equations is presented

in Chmielniak and Wróblewski (1995). At solid walls the non-slip condition is used for the viscous flow calculation. The pressure is found using the high Reynolds-number approximation. For the grid orthogonal to the walls it is:

$$\frac{\partial p}{\partial \eta} = 0. \tag{4.15}$$

Surface densities are computed from a specified wall temperature.

5. Numerical Results

Calculation processes were performed on the examples of blade systems of steam turbines. The application of the Godunov-type scheme for real geometry of turbomachinery was presented, with the application of various methods of discretisation and inviscid and viscous flow models.

5.1. 3-D inviscid flow calculations

Stator of the turbine

For test computations, the geometry of turbine stator was chosen. It is a fourth Standard Configuration proposed by Bölcs and Fransson (1986) for the workshop. This configuration was of interest mainly because it represents a typical modern turbine blades. This type of airfoil has relatively high blade thickness and chamber and operates under transonic flow conditions.

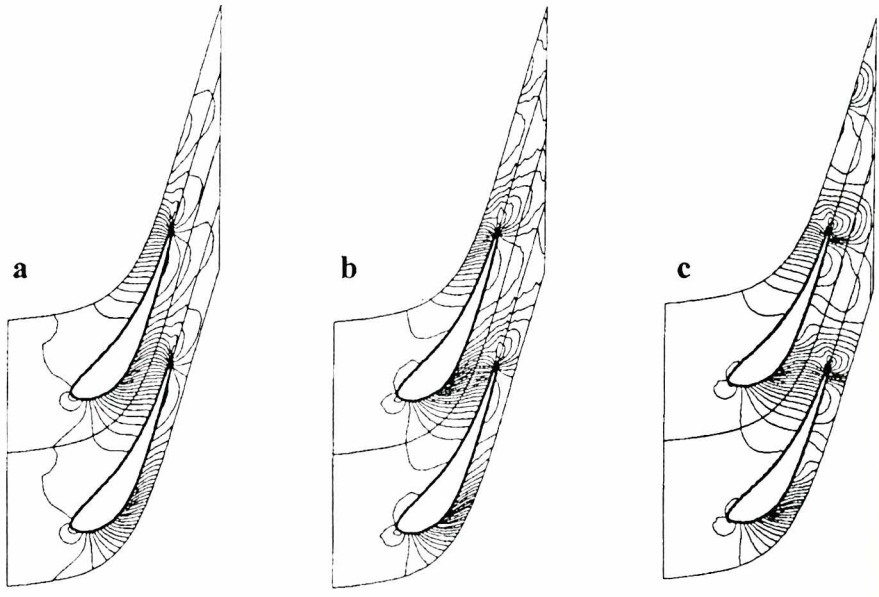

Figure 5.1 *The static pressure disribution, a) for the coarse grid and the first order accuracy scheme, b) for the coarse grid and the third order accuracy scheme, b) for the fine grid and the third order accuracy scheme*

The cascade configuration consists of 20 blades, each with a chord of $c = 0.0744$m with a maximum thickness-to-chord ratio of 0.17. The stagger angle is 56.6° with the pitch-to-chord ratio of the cascade 0.76. At the outlet, Mach number M = 1,19 was assumed. The numerical "*C*" type grid applied in computations contained 101×9×21 computation points for coarse grid and 201×17×21 for fine grid. The distributions of static pressure on the blade in average intersection of the blade high were presented in Figure 5.1. In the case of scheme of higher order, the structure of the resulting shock wave generated around the outlet edge was better, as it had been expected. The comparison of the distribution of Mach number on the profile shows considerable divergence of obtained results while applying different orders of accuracy, Figure 5.2. The results for the first order of accuracy on the

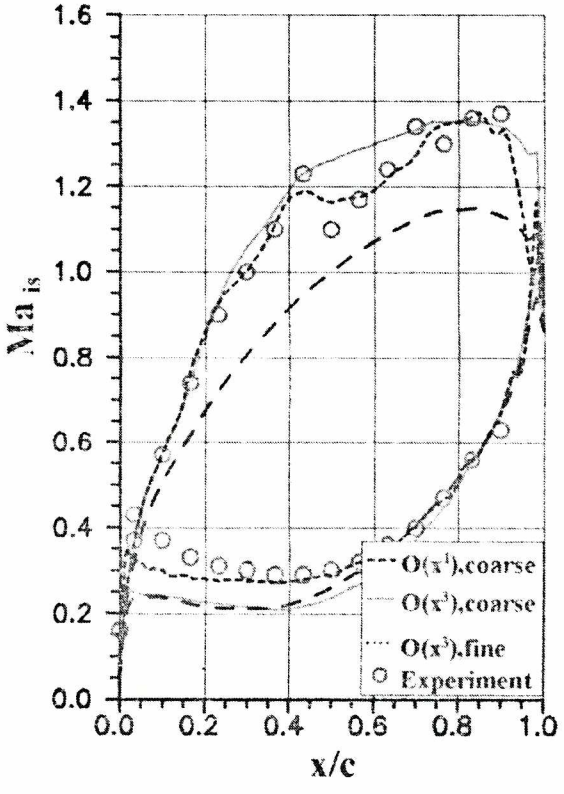

Figure 5.2 *Predicted and experimental Mach number distributions*

suction side differ considerably from the experiment results. The resolution improves in the case of scheme of higher accuracy order.

Stage of the steam turbine

The computation of low through the blade system of two blade-rings was carried out for the geometry of the last stage of the steam turbine. The geometry of this

stage is characterised by high blades and a small axial-ring gap. The calculations were carried out using the "*H*" grid type, which contained 65×15×27 computation nodes, both for the stator and the rotor (Figure 5.3). For the computation, the

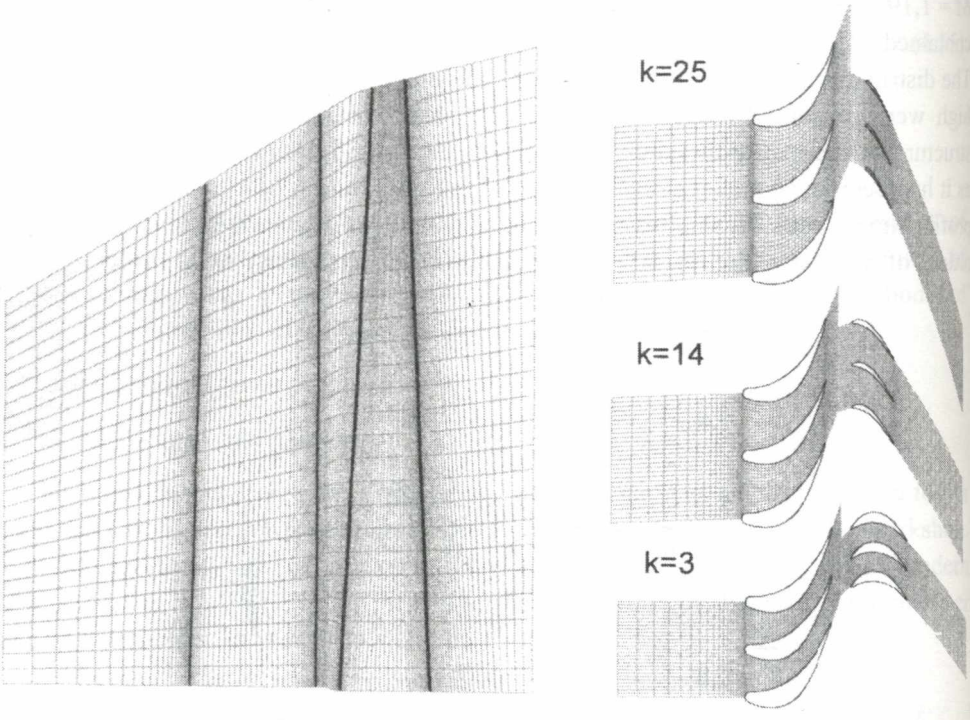

Figure 5.3 *"H"-type grid for the stage discretisation (k - grid surface number in r direction)*

numerical scheme of the third order of accuracy was applied. The stage under consideration works in the area of wet steam. For the computation the some combination of state equations for the perfect and real gas was applied. Distributions of the static pressure in the stage were presented in Figure 5.4. Applied boundary conditions, with defined parameters in the axial gap, made it possible to eliminate smoothly transfers from the absolute to the relative coordinate system. Strong wave structures generated around the outlet edge of the stator are modelled in the way eliminating the occurrence of reflections against the outlet boundary. In the case of stage computations, the number of iterations to solve Riemann problem at each grid cell face was controlled. When applying the optimal iteration process no more than 3 iterations were needed.

The application of the full Riemann problem requires longer computation time, but it may be attractive in the case of optimisation of the iteration process and in cases where strong wave phenomena occur, when detailed calculation of entropy changes is required.

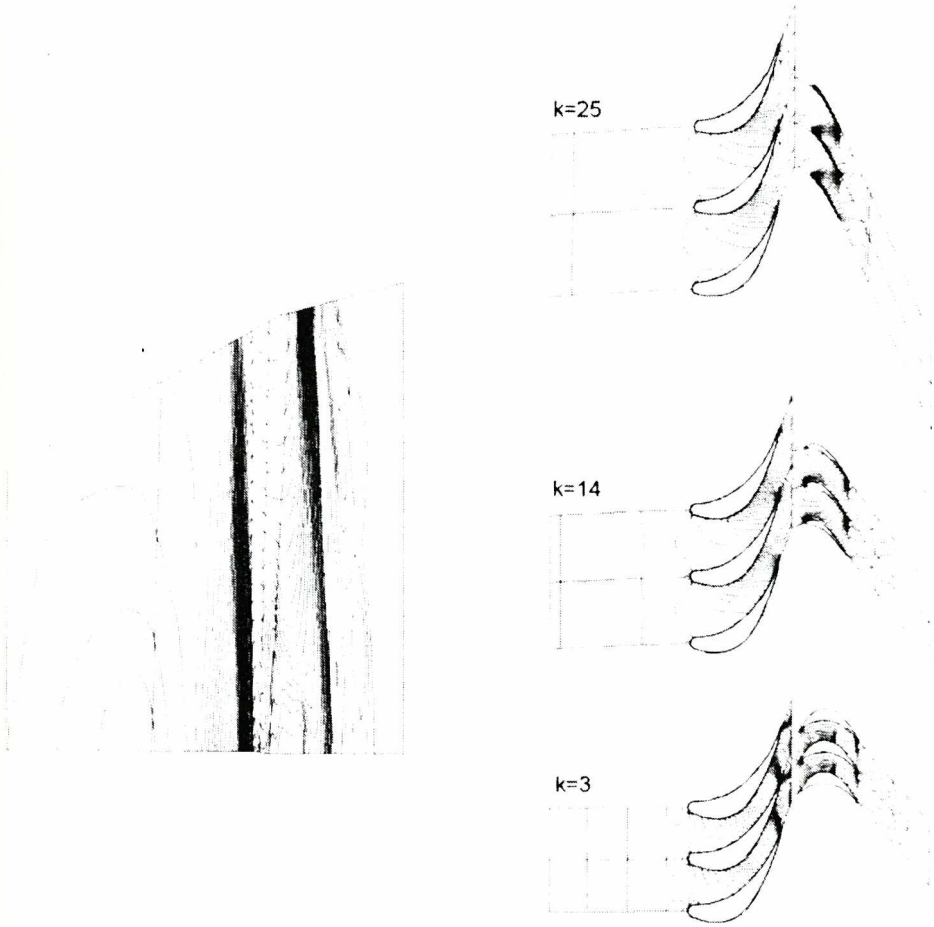

Figure 5.4 *Static pressure distributions for steam turbine stage (k - grid surface number in r direction)*

Stage of the experimental air turbine

The numerical calculation of the flow through an axial-flow turbine stage was performed. This turbine is an experimental turbine installed at the Technical University of Aachen (Gallus et al. 1990). All blades are prismatic, high turned and have relatively high thickness. The calculation domain was discretised using "*H*"-type mesh with 65×15×27 points for both stator and rotor blade cascade. An approximate Riemann solver was applied in the calculations. As an example of the calculations results static pressure isolines in chosen crosssections are presented (Figure 5.5)

5.2. 2-D viscous flow calculations

For the test computations a mid-section of the turbine stator blade cascade was chosen, for which parameters and experimental results were presented in Bölcs and Fransson (1986). Experiments are performed for many conditions from which two are chosen for comparison. There are two different regimes of the work: subsonic

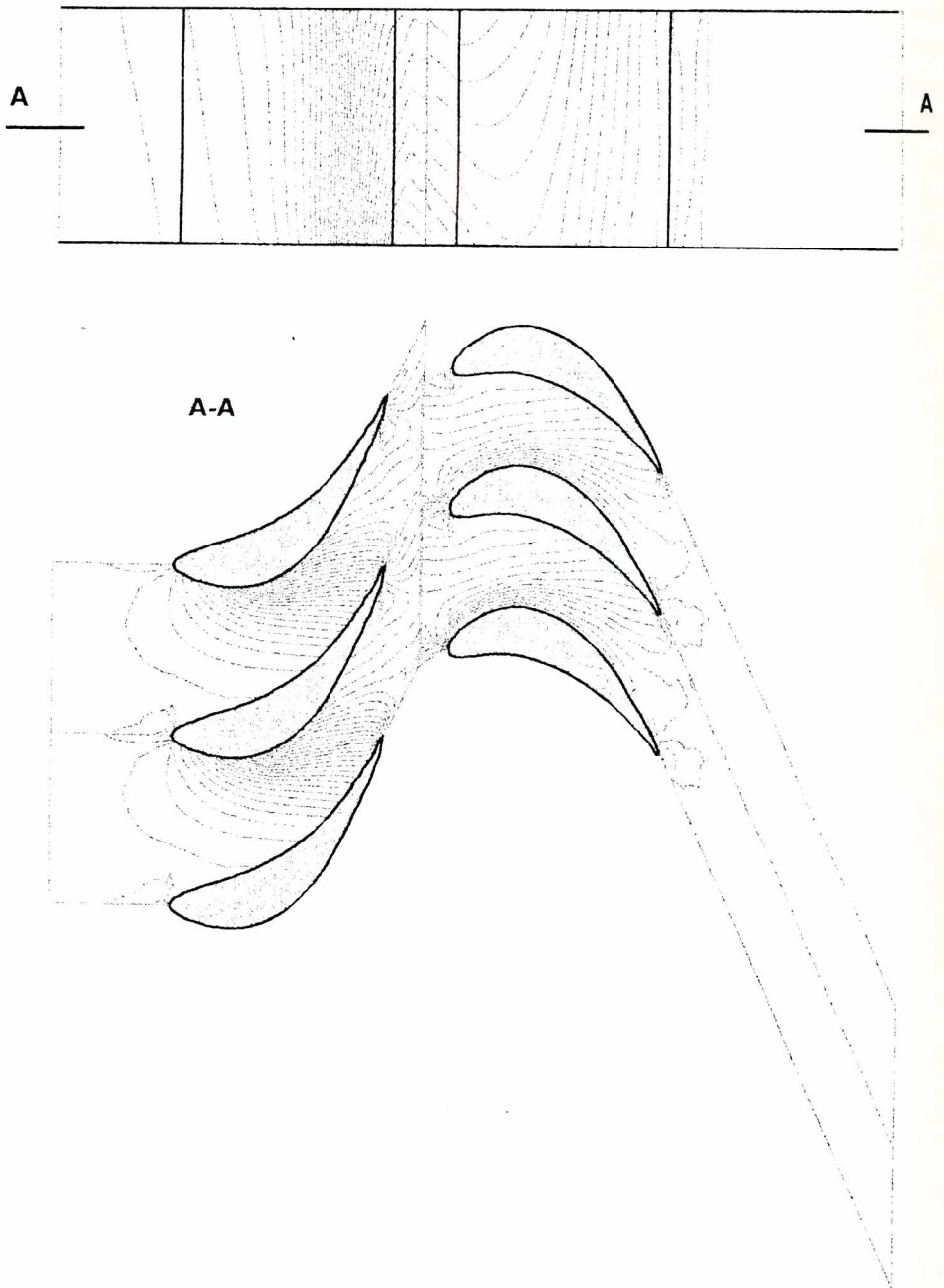

Figure 5.5 *Static pressure distributions for axial-flow air turbine stage (k - grid surface number in r direction)*

with the isentropic Mach number at the outlet $M_{2is} = 0.72$, and transonic with the Mach number $M_{2is} = 1.19$.

The computations are performed using the "*C*"-type grid with 401×33 nodes (Figure 5.6). A minimum grid line's distance at the wall was 0.03% of the chord

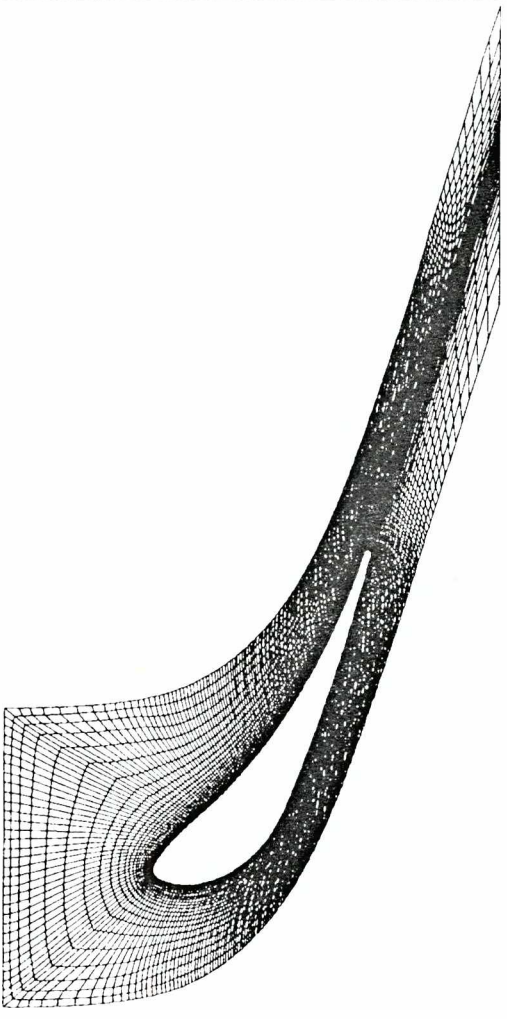

Figure 5.6 *"C"-type grid for the viscous flow computations*

length. In this case the chord Reynolds number based on the upstream conditions was $0.8 \cdot 10^6$, the Prandtl number and turbulent Prantdl number were 0.72 and 0.9, respectively.

Figure 5.7 shows the comparison of the experimental isentropic Mach number distribution and computed results. The good agreement of the calculated data with the experimental one is observed. Figure 5.8 shows the isolines of the Mach number distribution in the cascade.

The calculations with the same parameters except exit isentropic Mach number equal 1.19 are performed. The isentropic Mach number distribution obtained from the calculation is compared with experimental data in Figure 5.9. It is easy to recognise that the agreement between the calculated and measured data at the pressure side of the blade is very good. In the transonic and supersonic ranges at the

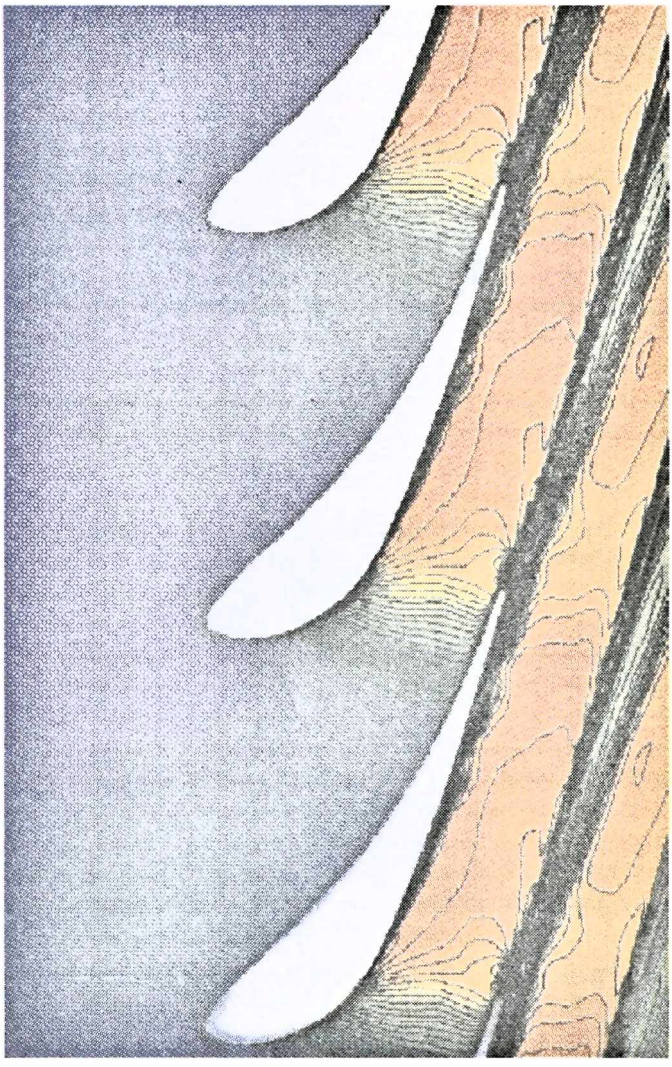

Figure 5.7 *Isentropic Mach number distribution (M_{2is} = 0.72)*

suction side the reflection of first shock wave generated at the trailing edge region is predicted well, but the second one is not present. This second shock wave reflection is obtained as a result of the two earlier reflections: first one from the suction side of the blade and second one from the wake region. On the numerical grid used for the calculations this second shock wave reflection at the suction side is smeared. The calculated isolines of the Mach number are displayed in Figure 5.10. The complex flow structure behind the trailing edge is presented in Figure 5.11.

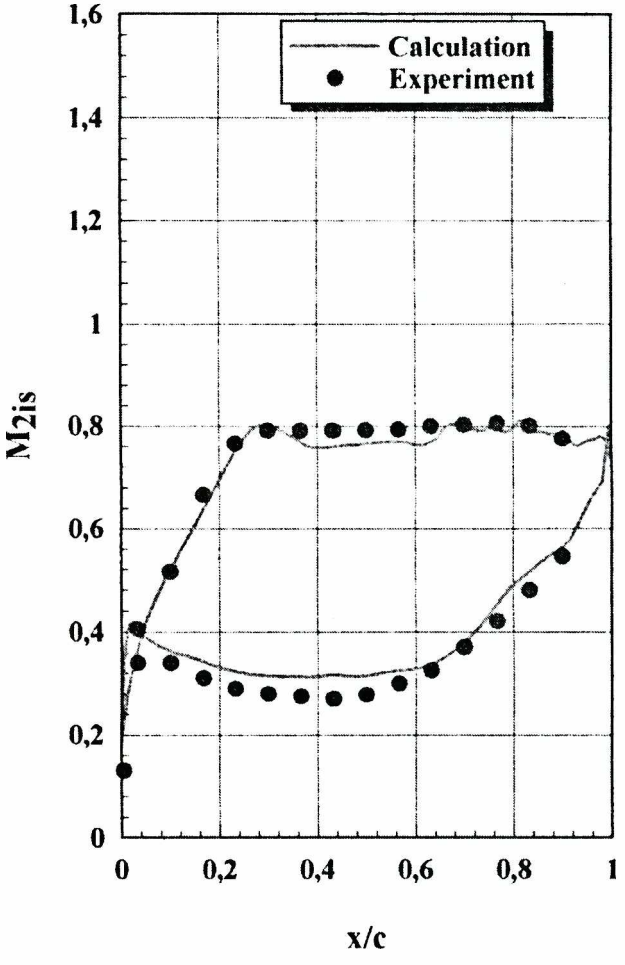

Figure 5.8 *Mach number contours (M_{2is}= 0.72)*

5.3. 2-D steam water flow calculations

Turbine stator

The calculations of the nucleating flow trough a turbine cascade were performed.The geometry of the last stage steam turbine stator was chosen. The non-ortogonal "*H*"-type grid with 71×21 mesh points was used. The convergence was reached for adiabatic flow after 6000 iterations and the diabatic flow required further 15000 iterations. The real gas calculations with nucleation phenomena is very time-consuming Calculations are 3-4 times longer than in the ideal gas model and the supercomputers are required especially in the 3D cases.

Figure 5.9 *Isentropic Mach number distribution (M_{2is} = 1.19)*

Figure 5.12 shows the adiabatic and diabatic pressure distribution on the blade profile. The discrepancies in pressure distributions when the condensation process occurred are observed. Figure 5.13. presents a non-equilibrium wetness rate contours in the blade cascade.

6. Concluding Remarks

A method of solving Euler and Navier-Stokes equations for turbomachinery cascades flows has been presented. These methods are based on an explicit time marching scheme. In the solution technique an upwind-biased discretisation of the

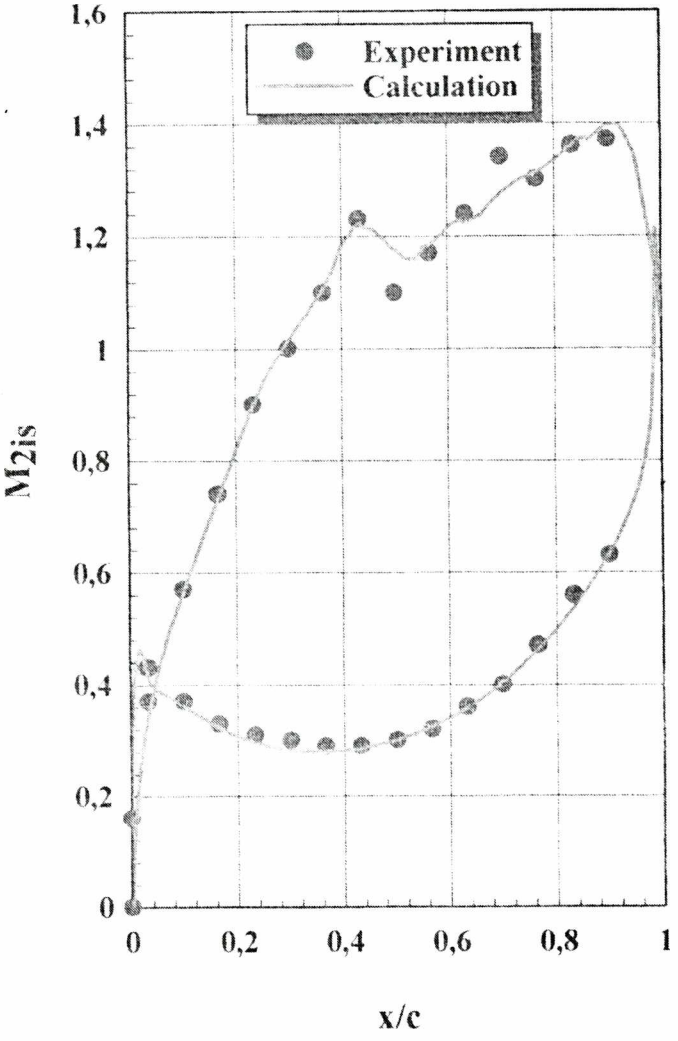

Figure 5.10 *Mach number contours (M_{2is}= 1.19)*

inviscid fluxes, thus avoiding additional artificial dissipation is used. The calculation is performed on the "*H*"-type grid and on the orthogonal "*C*"-type grid. The application of procedures of higher orders of accuracy in calculating of transonic flows better resolves the structure of discontinuity in the blade passages. The inviscid flow calculations show that the choice of scheme accuracy when the design problem is considered, could be very important. The viscous flow calculations are performed on the orthogonal "*C*"-type grid with implementation of the Baldwin-Lomax eddy-viscosity turbulence model. The more complex the flow structure is, the more complex the flow model has to be, and the more computer efficiency is required.

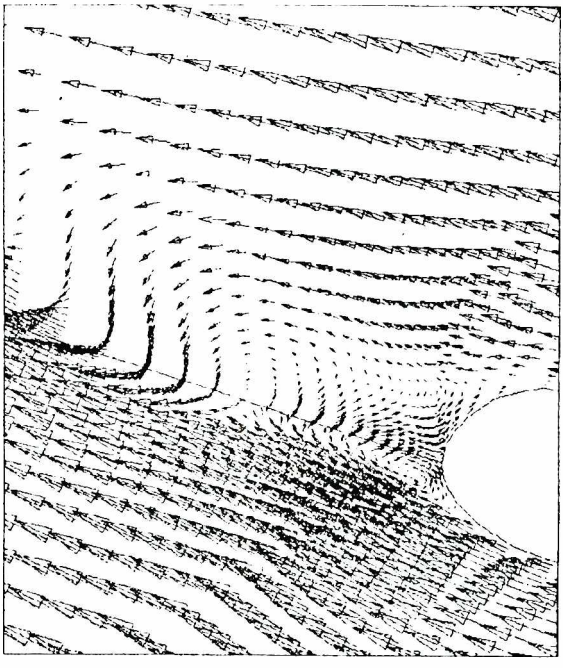

Figure 5.11 *Velocity vectors near the trailing edge*

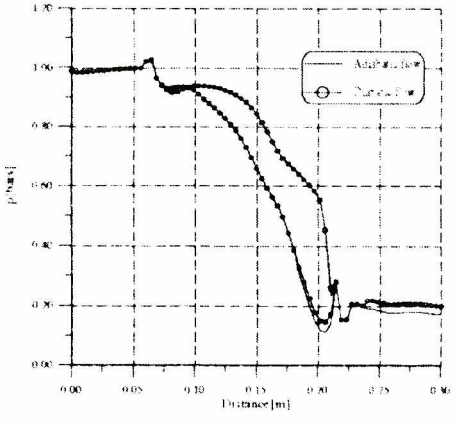

Figure 5.12 *Calculated pressure distribution on the blade profile (water steam)*

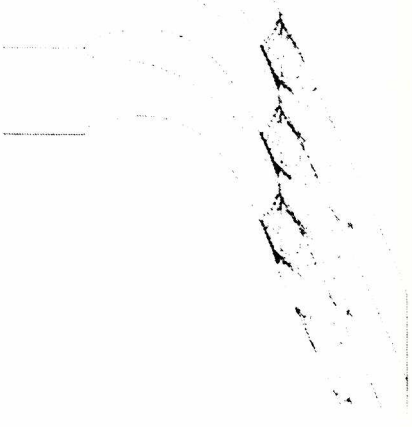

Figure 5.13 *Wetness rate contours*

The upwind method was implemented for calculations of the water vapour with homogeneous condensation. All described calculation results show very good ability of the upwind methods to model physical phenomena in blade cascades and that those methods are useful for engineering applications.

References

[1] Baldwin B. S., Lomax, H. (1978), *Thin Layer Approximation and Algebraic Model for Separated Turbulent Flow*, AIAA Paper, No. 78-257

[2] Benetschik H. (1991),*Numerische Berechnung der Trans- und Überschall-Strömung in Turbomaschinen mit Hilfe eines impliziten Relaxationsverfahren*, Dissertation, RWTH-Aachen

[3] Böles A., Fransson T.H., 1986, *Aeroelasticity in Turbomachines. Comparison of Theoretical and Experimental Cascade Results*. Communication du Laboratoire de Thermique Appliquee et de Turbomaschines de l'Ecole Polytechnique Federale de Lousanne, Nr 13

[4] Chakravarthy S. R. (1988), *High Resolution Upwind Formulations for the Navier-Stokes Equation*, VKI LS 1988-05

[5] Chien K. Y. (1982), *Prediction of Channel and Boundary-Layer Flows with Low-Reynolds-Number Turbulence Model*, AIAA Journal, Vol. 20, No. 1, pp. 33-38

[6] Chmielniak T. J., Wróblewski W., (1995), *Application of High Accuracy Upwind Schemes to Numerical Solution of Transonic Flows in Turbomachinery Blade Passage*, VDI-Berichte Nr 1185, pp. 63-77

[7] Chmielniak T. J., (1994) *Przeplywy transoniczne*, Ossolineum, Warszawa

[8] Chmielniak T. J., Wróblewski W., Dykas S. (1997), *Condensing Water Steam Flow in Expansion Channels, Modelling and Design in Fluid-Flow Machinery 1999*, Ed. J. Badur, J. Mikielewicz, Z. Bilicki, E. Oliwicki, Wydawnictwo IMP PAN, Gdansk

[9] Courant R., Isaacson E., Rees M., (1952) *On the Solution of Non-linear Hyperbolic Differential Equation*, Comm. Pure and Applied Math. pp. 243-255

[10] Deje M. E., (1981) *Gasdynamic of Two-Phase Flow*, Moscow (in Russian).

[11] Godunow S. K., (1976) *Cisliennoje rieszienie mnogomiernych zadac gazowoj dinamiki*, Nauka, Moskwa

[12] Godunov S. K., 1959, *A Difference Scheme for Numerical Computation of Discontinuous Solution of Hydrodynamic Equation*, Math. Sbornik, 47, pp. 271-306 (in Russian)

[13] Harten A., Hymann J. M., (1983), *Self Adjusting Grid Methods for One -Dimensional Hyperbolic Conservation law*, Journal of Computational Physics, Vol. 50, 235-269

[14] Hänel D., (1993), *Mathematische Stromungslehre*, Vorlrsungsumdruck des Aerodynamisches Institut der RWTH Aachen

[15] Hirsch C., 1990, *Numerical Computation of Internal and External Flows*, John Wiley and Sons, Chichester

[16] Jameson A., Schmidt W., Turkel E., (1981) *Numerical Solution of the Euler Equations by Finite Volume Methods Using Runge-Kutta Time Stepping Schemes*, AIAA Paper 81-1259

[17] Mac Cormack R. W., (1969) *The Effect of Viscosity in Hypervelocity Impact Cratering*, AIAA-Paper 69-354

[18] Lücke J. R., Benetschik H., Lohman A, Gallus H. E., (1995), *Numerical Investigation of Three-Dimensional Separated Flows Inside an Annular Compressor Cascade*,

Cieplne Maszyny Przepływowe, Zeszyt 108, Wyd. Politechniki Łódzkiej, pp. 227-237

[19] Manna M., (1992), *A Three Dimensional High Resolution Upwind Finite Volume Euler Solver*, VKI TN 180

[20] Merz R.,Krückels J., Mayer J. F., Stetter H., 1995, *Influence of Grid Refinement on the Solution of the Three-Dimensional Navier-Stokes Equations for Flow in a Transonic Turbine Stage with Tip Gap*, VDI-Berichte Nr 1185, pp. 211-224

[21] Osher S., (1984), *Riemann Solvers, the Entropy Condition and Difference Approximation*, SIAM Journal Numerical Analysis, 21, pp. 217,235

[22] Osher S., Solomon F., (1982), *Upwind Difference Schemes for Hyperbolic Systems of Conservation Laws*, Mathematics of Computation, Vol. 38, No. 158, pp. 339-374

[23] Pandolfi M., (1984), *A Contribution to the Numerical Prediction of Unsteady Flows*, AIAA Journal, Vol. 22, No. 5, pp. 602-610

[24] Pulliam T.H., (1986), *Artificial Dissipation Models for the Numerical Computation of Discontinuous Solutions of the Equations of Fluid Dynamics*, AIAA Journal, Vol. 24, No.12, pp. 1931-1940

[25] Roe P.L., (1981), *Approximate Riemann Solvers, Parameter Vectors and Difference Schemes*, Journal of Computational Physics, 43, pp. 357-372

[26] Saurel R., Larini M., Loraud J. C., (1994) *Exact and Approximate Riemann Solver for Real Gases*, Journal of Computational Physics, 112, pp. 126-137

[27] Schwane R., Hänel D., (1989), *An Implicit Flux-Vector Splitting Scheme for the Computation of Viscous Hypersonic Flow*, AIAA-Paper No. 89-0274

[28] Schnerr G., Dohrmann U., Jantzen H. A., Huber R. R., (1989) *Transsonische Stroemungen mit Relaxation und Energiezufuhr durch Wasserdampfkondensation*, Stroemungsmechanik und Stroemungsmaschinen, 40, pp. 39-79

[29] Sejna M., Lain J. (1994), *Numerical Modelling of Wet Steam Flow with Homogenous Condensation on Unstructured Triangular Meshes*, ZAMM 74, No. 5

[30] Steger J. L., Warming R. F., (1981), *Flux-Vector Splitting of the Inviscid Gas Dynamic Equations with Applications to Finite-Difference Methods*, Journal of Computational Physics, Vol. 40, pp. 263-293

[31] Sorenson R. L., (1980), *A Computer Program to Generate Two-Dimensional Grids About Airfoils and Other Shapes by the Use of Poisson's Equation*, NASA TM-81198

[32] Thompson J. F., Thames F. C., Mastin C. M., (1974), *Automatic Numerical Generation of Body-Fitted Curvilinear Coordinate System for Field Containing Any Number of Arbitrary Two Dimensional Bodies*, Journal of Computational Physics, 15, 1974, pp. 299-319

[33] Turner M. G., Jennions I. K., (1992), *An investigation of turbulence Modelling in Transonic Fans Including a Novel Implementation of an Implicit k-ε Turbulence Model*, ASME-Paper 92-GT-308

[34] van Albada G. D., van Leer B., Roberts W. W., (1982), *A Comparative Study of Computational Methods in Cosmic Gas Dynamics*, Astron. Astrophysics, 108, 76-84

[35] van Leer B., (1979), *Towards the Ultimate Conservative Difference Scheme. V.A Second order Sequel to Godunov's method*, Journal of Computational Physics, 32, pp. 101-136

[36] van Leer B., Thomas J. L., Roe P. L. and Newsome R. W., (1987), *A Comparison of Numerical Flux Formulas for the Euler and Navier-Stokes Equations*, AIAA Paper, No. 87-1104

[37] van Leer B., (1982), *Flux-Vector Splitting for the Euler Equations*, Lecture Notes in Physics, Vol. 170, pp. 507-512

[38] Wróblewski W.,Górski I. (1992), *Zastosowanie równan Poisson'a do generacji siatek dwuwymiarowych*, Opracowanie wewnętrzne Instytutu Maszyn i Urządzeń Energetycznych Pol. Śląskiej nr B-34/2, 1/92, Gliwice

[39] Wukalowicz M.P., Rivkin C.L., (1969) *Equations of State of the Superheated Water Vapour*, Teploenergetika, No 3, pp. 60-66 (in Russian)